Science and Technology Indonesia
*e*-ISSN:2580-4391 *p*-ISSN:2580-4405
Vol. 11, No. 2, April 2026

Research Paper

# Design and Formulation of Hydrogel Sponges for Mesenchymal Stem Cell Secretome Delivery

Deni Noviza[1*], Syahda Permata Ardelia[2], Marlina[2]

[1]*Department of Pharmaceutics, Faculty of Pharmacy, Universitas Andalas, Kampus Unand Limau Manis, Padang, West Sumatra, 25163, Indonesia*
[2]*Department of Chemical Pharmacy, Faculty of Pharmacy, Universitas Andalas, Kampus Unand Limau Manis, Padang, West Sumatra, 25163, Indonesia*
***Corresponding author**: deninoviza@phar.unand.ac.id*

**Abstract**
The mesenchymal stem cells (MSCs) secretome plays multiple roles in tissue regeneration and wound healing due to its content of various bioactive factors, including Fibroblast Growth Factor-2 (FGF-2). To support its topical application, an effective delivery system is required to preserve the stability and bioactivity of the secretome. A hydrogel sponge based on PVA-HPMC-PEG was selected as the delivery matrix due to its porous structure, flexibility, and ability to release active substances, thereby making it a promising candidate for wound healing applications. The objective of this research was to formulate a PVA-HPMC-PEG-based hydrogel sponge for a secretome delivery system. The hydrogel sponge was prepared using the freeze-drying method and optimized by varying the PVA concentration to achieve the desired physicochemical characteristics. The optimal formulation (F4) consists of 20% PVA, 2% HPMC, and 7.5% PEG. Evaluation revealed that this formulation exhibited a flexible sponge-like structure with a swelling percentage of 279.793% ± 0.06, elongation percentage of 107.923% ± 4.98, and physical crosslinking confirmed by FTIR analysis. Scanning Electron Microscopy (SEM) analysis demonstrated pore size ranging from 20 to 215 $\mu$m. Furthermore, secretome release was assessed using a Franz diffusion cell, and FGF-2 levels were quantified via ELISA. The results confirmed that the hydrogel sponge effectively facilitated the release of the secretome.

**Keywords**
Secretome, Hydrogel Sponge, PVA-HPMC-PEG, FGF-2, ELISA

Received: 17 December 2025, Accepted: 2 March 2026
https://doi.org/10.26554/sti.2026.11.2.692-700

## 1. INTRODUCTION

Stem cells are undifferentiated cells capable of differentiating into various specialized cell types. Among them, mesenchymal stem cells (MSCs) have attracted significant interest due to their broad potential in regenerative medicine. MSCs have been shown to promote cartilage and bone repair, enhance wound healing, and support cardiac and neural regeneration, in addition to their immunomodulatory properties (Widowati et al., 2025). MSCs accelerate chronic wound healing by improving epithelialization, stimulating tissue formation, and inducing neovascularization (Caplan, 2018).

The therapeutic effects of MSCs are primarily mediated by their secretion of bioactive molecules, collectively referred to as the MSC secretome (Ibrahim et al., 2022). This secretome includes cytokines, chemokines, growth factors, immunomodulatory molecules, microvesicles, and exosomes. Among the growth factors, Fibroblast Growth Factor-2 (FGF-2) plays a central role in promoting proliferation, angiogenesis, and tissue regeneration (Farooq et al., 2021). Secretome-based therapy offers several important advantages over direct cell therapy, including a reduced risk of immune rejection, improved stability and safety, lower costs, and greater flexibility in therapeutic delivery (Foo et al., 2021).

Despite these advantages, the delivery of secretome remains challenging. Bioactive factors are highly susceptible to enzymatic degradation, often requiring high or repeated dosing to achieve therapeutic efficacy (Yim et al., 2019). Moreover, systemic administration by injection can lead to rapid distribution into non-target organs, increasing the risk of cytotoxicity (Lai et al., 2014; Suresh et al., 2020). These limitations highlight the need for a localized delivery system that can protect the secretome, maintain its bioactivity, and ensure sustained therapeutic action at the target site as wound healing.

Previous studies have reported the development of secretome -based formulations in various delivery systems, including gels formulated with polyisocyanate (PIC) polymers (Liu et al., 2020), hydrogels composed of carrageenan and polyvinyl alcohol (Robert et al., 2019), Pluronic®F127 (Wang et al.,

2019), chitosan (Nooshabadi et al., 2020) and Carbopol (Widowati et al., 2025). Furthermore, secretome has been incorporated into advanced delivery platforms such as in situ gels and thermal sensitive hydrogel (Zhang et al., 2022), pH-sensitive hydrogels (Li et al., 2021), and electrospun scaffolds (Deshpande et al., 2018). Although these drug delivery systems have demonstrated effectiveness in wound healing, their application remains limited by a short residence time at the wound site, as they are readily washed away.

Wound dressing has long been recognized as a crucial strategy in the management of chronic wounds. However, conventional approaches such as traditional bandages, hydrogels, and foam dressings exhibit several limitations in wound care, including their inability to adapt to dynamic wound progression and limited applicability for wounds located in joint areas (You et al., 2024). Consequently, current research has increasingly shifted toward the development of innovative wound dressings capable of actively facilitating the healing process by triggering one or more phases of the natural wound healing process.

Among the modern wound dressings, hydrogel sponges have emerged as particularly promising candidates (Qiao et al., 2023). Their porous, three-dimensional hydrophilic network enables high water absorption and biocompatibility (Zhang et al., 2013; Zhang and Zhao, 2020), while their flexibility, non-adhesive nature, and structural similarity to living tissue make them suitable as wound dressings (Francesko et al., 2018; Li et al., 2020).

Incorporating growth factors or bioactive molecules into hydrogel matrices has been shown to enhance wound healing outcomes (Shi et al., 2017). Polymers such as polyvinyl alcohol (PVA) (Ng et al., 2014), hydroxypropyl methylcellulose (HPMC) (Ghorpade et al., 2016), and polyethylene glycol (PEG) (Durairaj et al., 2024) are widely used to optimize hydrogel properties, improving mechanical strength, elasticity, and swelling capacity. Previous studies have investigated PVA-HPMC-PEG hydrogels for wound healing (Li et al., 2020), however, their application as carriers for secretome delivery has not yet been explored. Addressing this gap, the present study aims to develop and evaluate a PVA-HPMC-PEG–based hydrogel sponge as a localized delivery system for MSC secretome.

## 2. EXPERIMENTAL SECTION

### 2.1 Materials

The materials used in this study included adipose-derived mesenchymal stem cells (ADMSCs) (Merck®, Germany), polyvinyl alcohol (PVA) (Chang Chun®, China), hydroxypropyl methylcellulose K4M (HPMC) (FPP, Indonesia), polyethylene glycol 2000 (PEG 2000) (Sigma Aldrich®, USA), deionized water (Onemed®, Indonesia), 0.45 µm MCE membrane filters (MF-Millipore$^{TM}$, USA), Dulbecco's Modified Eagle Medium (DMEM) (Gibco®, USA), fetal bovine serum (FBS) (Gibco®, USA), phosphate-buffered saline (PBS) (Merck®, Germany), trypsin-EDTA, trypan blue, antibiotic solution containing penicillin (10,000 units/mL) and streptomycin (10,000 $\mu$g/mL) (Gibco®, USA), sterile distilled water, 70% ethanol, and a human FGF-2 ELISA Kit (Elabscience®, USA).

### 2.2 Intrumentation

The research instruments employed in this study are as follows: incubator (ARA®P170, South Korea), magnetic stirrer (IKA®C-MAG HS 7, Germany), freeze drying (Buchi®Lyovap or L-200, Switzerland), tensile tester (A&D Company®Tensilo n RTI-1310, Japan), Scanning Electron Microscopy (SEM) (Jeol®, JSM-6510LA, Japan), and Fourier-Transform Infrared Spectroscopy (FTIR) (Thermo Scientific®Nicolet iS10, USA).

### 2.3 Methods

#### 2.3.1 Preparation of Culture Medium

The culture medium was prepared by supplementing Dulbecco's Modified Eagle Medium (DMEM) with 20% fetal bovine serum (FBS) and 1% penicillin-streptomycin antibiotic solution. The prepared medium was sterilized by aliquoting and stored at -20°C until use. Prior to use, the medium was thawed and pre-warmed to 37°C (Marlina et al., 2023).

#### 2.3.2 Cell Culture Expansion

Adipose-derived mesenchymal stem cells (ADMSCs) stored at -80°C were thawed in a 37°C water bath (Cleaver Scientific®SWB -10L-1, UK) for approximately 2 minutes, followed by centrifugation (Hanil®M15R, South Korea) at 2000 rpm for 2 minutes. The resulting cell pellet was resuspended in 1 mL of culture medium and transferred into a flask. Cells were incubated at 37°C in a 5% $CO_2$ incubator (ARA®P170, South Korea), with medium changes every 2–3 days. Upon reaching 80–90% confluency, cells were washed with phosphate-buffered saline (PBS), treated with 1 mL trypsin-EDTA for 5 minutes, and the reaction was neutralized by adding fresh medium. Cells were then centrifuged and resuspended in new medium, followed by subculturing into two flasks for further expansion.

#### 2.3.3 Secretome Collection and FGF–2 Analysis

The secretome was collected from MSC cultures that reached 80-90% confluency. The culture medium was filtered through a spray filter 0.22 $\mu$m membrane (TPP®, Switzerland) to remove cellular debris and stored at -20°C. The FGF-2 content was quantified using a Human FGF-2 ELISA Kit (Elabscience®, USA), following the manufacturer's instructions (Elabscience Biotechnology Co., Ltd., n.d.; Marlina et al., 2023).

#### 2.3.4 Hydrogel Sponge Formulation

The hydrogel sponge was formulated by varying concentrations of PVA and combining it with HPMC and PEG in deionized water (Table 1).

PVA at the specified concentrations was dispersed in 30 mL of deionized water using a magnetic stirrer (IKA®C-MAG HS 7, Germany) at 85°C for 60 minutes until fully dissolved. Separately, 2% HPMC was dispersed in 30 mL of deionized water until homogeneously mixed. The two solutions were then

**Table 1.** The Hydrogel Sponge Formulation

| Materials | Concentration (%) | | | |
|---|---|---|---|---|
| | F1 | F2 | F3 | F4 |
| PVA | 5 | 10 | 15 | 20 |
| HPMC | | 2 | | |
| PEG | | 7.5 | | |

combined in a 1:1 ratio and stirred until a uniform mixture was achieved. PEG was subsequently added to the mixture and stirred until homogeneous. The final mixture was poured into molds, frozen for 12 hours, and subjected to freeze drying (Buchi® Lyovapor L-200, Switzerland) at -57°C under 0.3 Mbar pressure until it was completely dried and had a sponge-like structure (Li et al., 2020).

#### 2.3.5 Evaluation of Hydrogel Sponge Formulation

The hydrogel sponge formulations were evaluation for organoleptic, swelling test, and texture analysis. Visual observation was conducted to assess the physical characteristics and appearance of the hydrogel sponge. Subsequently, a swelling test was performed by immersing the hydrogel sponge in water at room temperature, and the percentage increase in weight was calculated using Equation (1) (Pandey et al., 2020; Song et al., 2017).

$$\text{Swelling (\%)} = \frac{M_1 - M_0}{M_0} \times 100\% \quad (1)$$

where $M_0$ is the initial dry weight, and $M_1$ is the weight after swelling. Meanwhile, texture analysis was performed to assess the mechanical properties of the sponge using a tensile tester following ASTM D638 standards. Samples were pulled at a rate of 10 mm/min to determine tensile strength, elongation, and elastic modulus (Li et al., 2020). Based on the organoleptic evaluation, swelling test, and texture analysis, an optimum formulation was identified and subsequently subjected to further characterization, including Scanning Electron Microscopy (SEM) and Fourier-Transform Infrared Spectroscopy (FTIR) analyses. SEM was employed to examine the surface morphology of the hydrogel sponge, with micrographs recorded at magnifications of 200× and 500× (Bal-Ozturk et al., 2019).

#### 2.3.6 Evaluation of FGF-2 Content in Secretome-Loaded Hydrogel Sponge

The FGF-2 content was analyzed using a Human FGF-2 ELISA kit, following the manufacturer's instructions. Hydrogel samples (1.5 cm diameter) were incubated with MSC secretome for 15 minutes in room temperature prior to secretome release test. The pre-soaked sponge was placed on a cellulose acetate membrane in a Franz diffusion cell (modification) device containing PBS (pH 7.4) at 37°C. After 6 hours, the medium was collected, and the concentration of the FGF-2 was quantified using ELISA (Van De Sandt et al., 2004).

Meanwhile, sponge incubation medium evaluation was conducted by incubated secretome-loaded sponge samples in PBS (pH 7.4) at 37°C until fully dissolved, after which the solution was collected and analyzed for FGF-2 content by ELISA (Kwon et al., 2023).

## 3. RESULTS AND DISCUSSION

### 3.1 Secretom Isolation

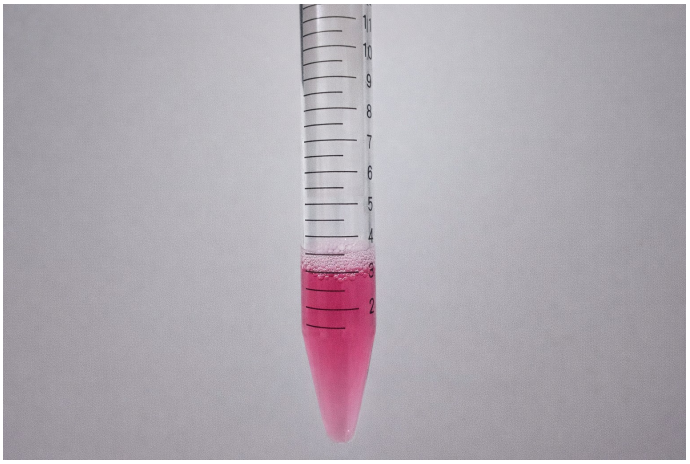

**Figure 1.** Secretom

Mesenchymal Stem Cells (MSCs) are a type of multipotent stem cell widely studied for their capacity to differentiate and secrete various bioactive components that support tissue regeneration. In the context of wound healing, MSCs exhibit therapeutic effects through the secretion of a complex mixture into their culture medium, known as the secretome. This secretome contains cytokines, chemokines, growth factors, and exosomes, which synergistically accelerate epithelialization and angiogenesis, while suppressing inflammation and apoptosis in wounded tissue (Chu et al., 2019).

One of the key components of the MSC secretome is Fibroblast Growth Factor-2 (FGF-2), which plays a significant role in stimulating fibroblast proliferation, enhancing collagen synthesis, and promoting skin tissue regeneration (Farooq et al., 2021).

MSC culture was performed using DMEM medium supplemented with 20% FBS to meet the nutritional requirements during cell growth, along with the addition of penicillin-streptomycin to prevent contamination (Zhang et al., 2013; Yao and Asayama, 2017). Once the cultured cells reached confluency, the medium was collected and filtered using a 0.22 $\mu$m membrane to remove cellular debris. This filtered medium is referred to as the secretome (Figure 1). The secretome obtained appears pink due to the presence of phenol red, a pH indicator commonly added to culture media such as DMEM; therefore, the coloration is not attributable to the secretome itself.

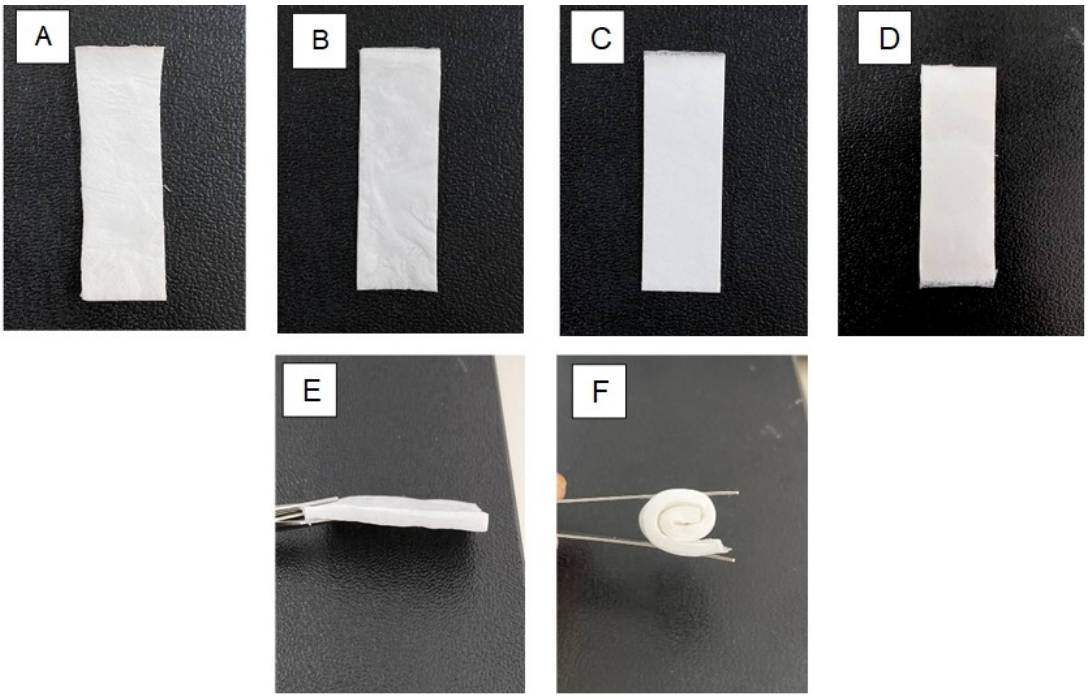


**Figure 2.** Organoleptic Observation of Hydrogel Sponge Surface from Various Formulations: (A) F1, (B) F2, (C) F3, (D) F4, (E) Side View and (F) Flexibility Assessment of Hydrogel Sponge

**Table 2.** Mechanical Properties of Hydrogel Sponge Formulations

| Formulation | Elastic modulus (MPa) | Max point extension (mm) | Max point elongation (%GL) | Max point stress (MPa) |
|---|---|---|---|---|
| F3 | – | 37.81 ± 17.29 | 34.84 ± 12.87 | 0.011 ± 0.005 |
| F4 | 0.039 ± 0.02 | 123.34 ± 5.28 | 107.92 ± 4.98 | 0.048 ± 0.03 |

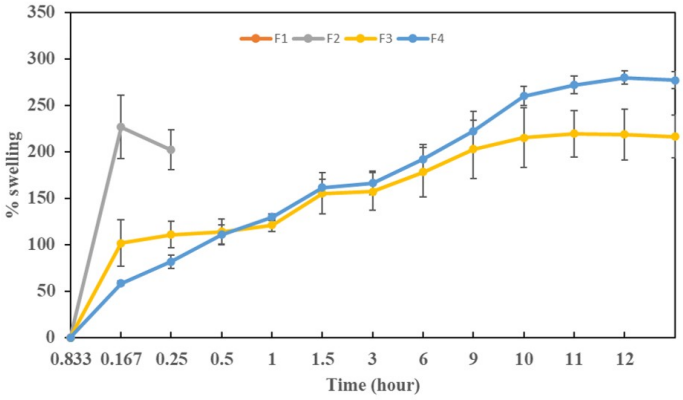


**Figure 3.** Swelling Profile of Hydrogel Sponge Formulation Over Time

### 3.2 Hydrogel Sponge Formulation

Porous hydrogel sponges are capable of absorbing the secretome and delivering it to the target site. In this formulation, the polymers used were PVA, HPMC, and PEG. PVA, as the primary polymer, provides mechanical strength and structural stability to the sponge. HPMC acts as a porogen and enhances the swelling capacity (Yu et al., 2024), while PEG functions as a plasticizer and pore-forming agent, contributing to the formation of a smooth porous structure (Li et al., 2020).

This study formulated four hydrogel sponge variants by varying the concentration of PVA to identify the optimal formula. After preparing the polymer blends according to the predetermined formulations, the mixtures underwent a freeze-drying process to remove water content without transitioning the material into a liquid phase, thus preserving the structure and stability of the sponge. Visually, all four formulations (F1–F4) exhibited similar appearances (Figure 2), characterized by a white color, homogeneous texture, and a sponge-like structure. The optimal formula was selected based on organoleptic evaluation, swelling capacity, and mechanical characteristics.

### 3.3 Evaluation of Hydrogel Sponge Formulation

Swelling capacity was then evaluated, as it plays a crucial role in determining the sponge's ability to absorb and deliver active substances. Based on the data in Figure 3, F1 and F2 displayed structural instability during the initial swelling test and disinte-

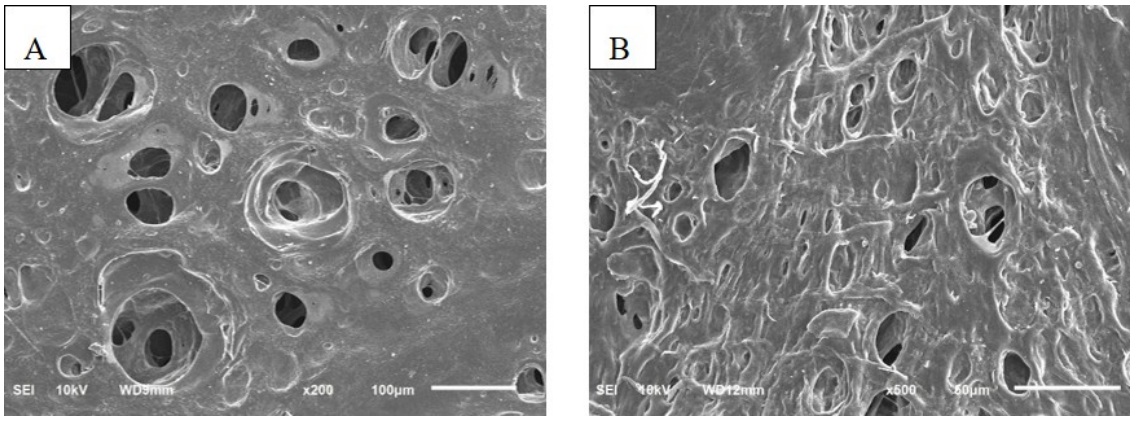


**Figure 4.** SEM Images of Hydrogel Sponge: (A) Surface Morphology at 200× Magnification and (B) Cross-Sectional Morphology at 500× Magnification

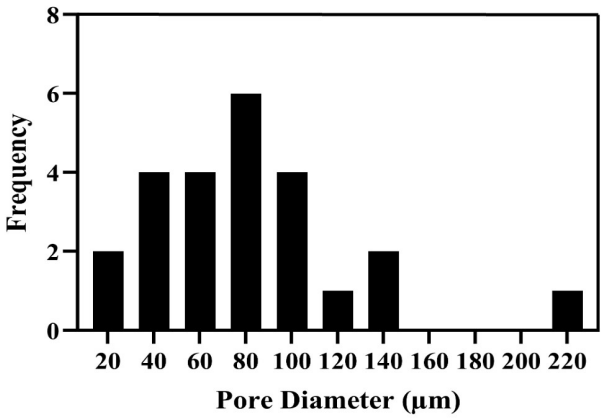


**Figure 5.** Pore Size Distribution on the Surface of Hydrogel Sponge as Shown by Histogram Analysis

grated rapidly due to the low PVA content, and were therefore excluded from the selection of the optimal formula.

In contrast, F3 and F4 maintained their structural integrity during the swelling test. F4 remained stable for up to 11 hours and demonstrated the highest absorption capacity, 279.79% ± 0.06, compared to F3 at 220.34% ± 0.53. Statistically, F4 showed a significantly superior ability to absorb and retain its structural integrity, as indicated by an independent samples t-test (p = 0,019, $p$ <0,05).

The swelling ratio of F4 was lower than that reported in the literature, which can be attributed to differences in polymer composition. Carboxymethyl cellulose (CMC), for instance, exhibits higher hydrophilicity than HPMC, which contributes to a lower swelling capacity in F4 (Dharmalingam and Anandalakshmi, 2019). Despite the lower value, the sponge still falls under the classification of high-swelling hydrogels, making it suitable for wound healing applications (Feng and Wang, 2023).

Subsequently, the mechanical properties of the optimal formula were assessed using a Universal Testing Machine (UTM), as mechanical strength is critical for maintaining sponge integrity during application and preventing tearing or deformation on wounded or intact skin (Spicer, 2020).

The mechanical testing procedure followed ASTM D638, a standard method for measuring the tensile properties of polymeric materials (American Society for Testing and Materials, 2016). As shown in Table 2, F4 demonstrated the highest elongation at 107.92% ± 4.98, compared to F3 at 34.84% ± 12.87, indicating greater elasticity and flexibility during use. F4 also exhibited a higher maximum point extension (123.34 mm) than F3 (37.81 mm), confirming its superior stretchability before breakage. In addition, F4 had a higher tensile strength (0.048 MPa) than F3 (0.011 MPa). Notably, F4 was the only formula with a measurable modulus of elasticity (0.0395 ± 0.02 MPa), while F3 failed to register due to being too fragile during testing. These findings reinforce F4's superior mechanical properties, particularly in terms of flexibility and structural integrity, during application.

Compared to a study by Li et al. (2020), which reported a higher tensile strength using a PVA-CMC-PEG combination (0.20 MPa), the lower tensile strength in this study can be attributed to the use of HPMC. While HPMC is more elastic, it does not contribute significantly to tensile strength (Du et al., 2025). However, its ability to enhance elongation makes F4 superior in terms of flexibility and user comfort. Overall, the evaluation confirms that F4 is the most optimal formulation for further characterization.

The selected optimal formula (F4) was further characterized using SEM to observe surface morphology and FTIR to evaluate the interaction between polymers. SEM analysis (Figure 4) examined both surface and cross-sectional morphology. The results showed that the hydrogel sponge had a porous structure with varied pore sizes formed due to ice sublimation during freeze-drying. The surface displayed multilayered pores that extended into the matrix, potentially enhancing fluid diffusion and the release of active substances. The cross-sectional

**Table 3.** FGF-2 Detection Results in Secretome and Formulations

| Sample | Absorbance | | Mean ± SD | FGF-2 Concentration (pg/mL) | % Recovery |
|---|---|---|---|---|---|
| | 1 | 2 | | | |
| Secretome | 0.174 | 0.174 | 0.174 ± 0.0002 | 224.929 | – |
| Hour release | 0.039 | 0.031 | 0.035 ± 0.005 | 26.214 | 740.542 |
| Direct incubation media | 1.050 | 1.045 | 1.047 ± 0.003 | 1472.428 | 41595.93 |

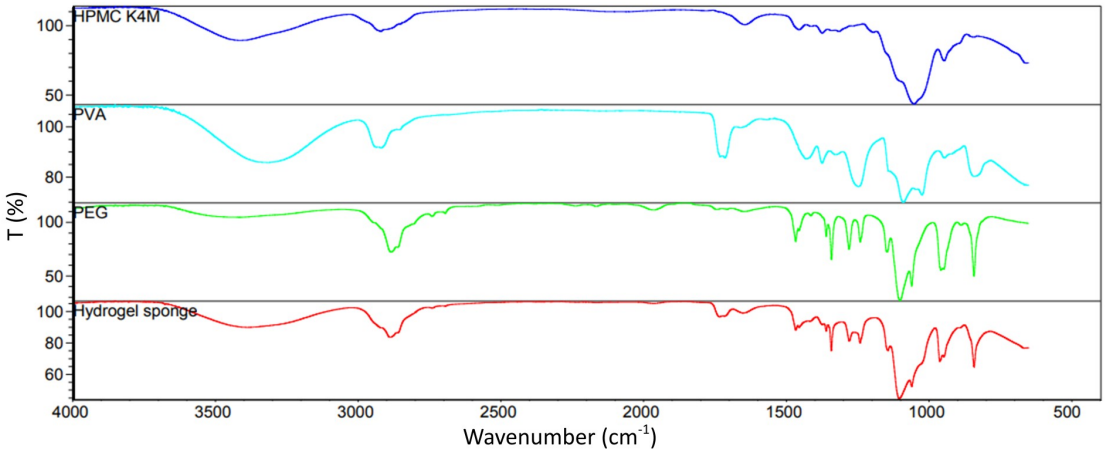


**Figure 6.** FTIR Spectrum of Hydrogel Sponge

**Table 4.** Interference Analysis of Hydrogel Sponge without Secretome on ELISA

| Sample | Absorbance | | Mean ± SD |
|---|---|---|---|
| | 1 | 2 | |
| PBS | 0.0145 | 0.011 | 0.0128 ± 0.0002 |
| PBS + hydrogel sponge | 0.9709 | 1.0355 | 1.0032 ± 0.0045 |

view revealed a uniform distribution of pores of various sizes throughout the sponge's thickness.

ImageJ analysis revealed the pore size distribution (Figure 5) ranged from 20 to 215 $\mu$m. This variation contributes to the sponge's physical properties, such as swelling capacity and mechanical stability. Compared to literature values, the pore sizes are within a comparable range, though slightly broader. Shi et al. (2017) reported surface pores of 50–150 $\mu$m and cross-sectional pores of 200–500 µm, while Li et al. (2020) found pore sizes between 30–140 $\mu$m. These differences are attributed to variations in polymer composition and freezing conditions.

In this study, pre-freezing was performed at -20°C, a temperature known to produce larger ice crystals and thus a broader pore size distribution (Podhorská et al., 2020). This explains the variation and size distribution of pores observed in the hydrogel sponge.

Overall, the diverse and multilayered pore structure of the hydrogel sponge supports an effective balance between absorption and controlled release of the secretome, making it a suitable candidate for topical delivery systems and wound dressing applications.

The FTIR analysis was then conducted to identify functional groups and observe potential crosslinking among the polymers. The spectra (Figure 6) showed no significant new peaks in the hydrogel sponge spectrum compared to the individual polymer spectra, suggesting that no chemical bonds were formed. Instead, the interactions among polymers were physical in nature.

### 3.4 Evaluation of FGF-2 Content in Secretom Loaded Hydrogel Sponge

In this study, FGF-2 content in the secretome was quantified using ELISA, considering FGF-2's critical role in promoting cell proliferation for wound healing (Farooq et al., 2021). The concentration of FGF-2 in the secretome was found to be 224.93 pg/mL. The secretome was then incorporated into the

hydrogel sponge, and a release study was performed using a Franz diffusion cell.

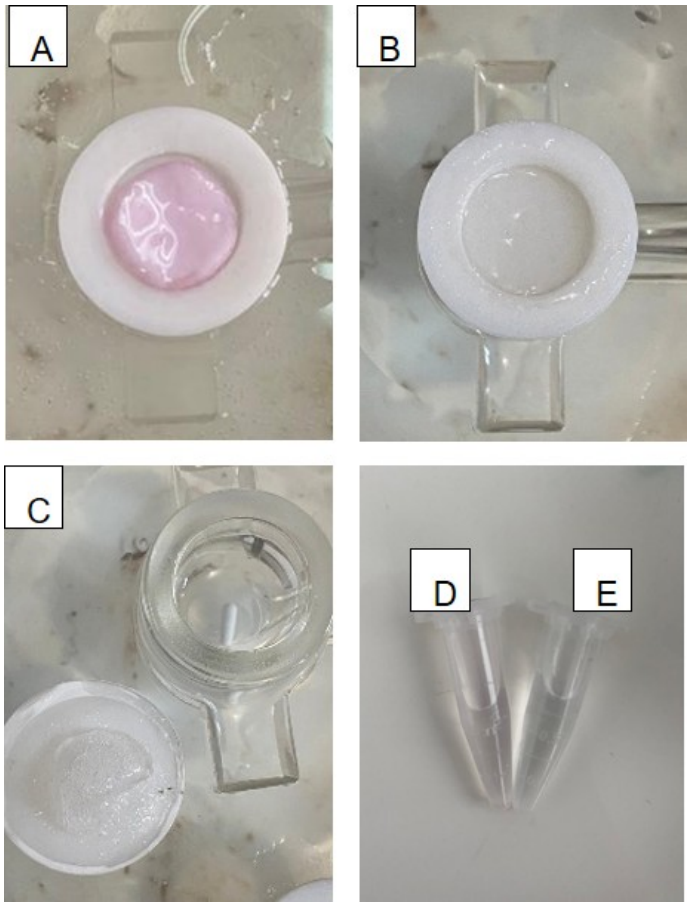


**Figure 7.** Visual Observation of the Hydrogel Sponge Before and After Secretome Release, and the Corresponding Incubation Media. (A) Hydrogel Sponge Prior to Release; (B-C) Hydrogel Sponge Post-Release; (D) Incubation Medium Following Sponge Dissolution; (E) Phosphate-Buffered Saline (PBS) Ph 7.4

Visually, changes in color observed in both the sponge and the incubation medium (Figure 7) indicated the release of active compounds. However, ELISA results (Table 3) showed unexpectedly higher FGF-2 levels in the release and incubation media up to 1472.43 pg/mL than in the original secretome. This prompted further investigation into potential matrix interference.

A control experiment (Table 4) revealed that pure PBS had low absorbance, whereas PBS combined with a blank sponge (without secretome) exhibited high absorbance (1.0032). This interference likely resulted from non-specific interactions between the sponge polymers and antibodies in the ELISA wellplate, causing false-positive signals and inflated absorbance readings (Tate and Ward, 2004). This phenomenon, known as matrix interference, has also been reported in previous studies, such as those by Jiang et al. (2021), which found that non-biological components can lead to false-positive results in ELISA, as ELISA is typically validated for use only with biological fluids. Additional validation is therefore necessary when ELISA is applied to polymer-based matrices, such as hydrogel sponges.

## 4. CONCLUSIONS

This study demonstrates that a PVA-HPMC-PEG-based hydrogel sponge was successfully formulated as a delivery system for MSC secretome in topical wound healing applications. Formula F4 was selected as the optimal formulation due to its high swelling capacity, good elasticity, and multilayered porous structure with a size distribution conducive to secretome diffusion. FTIR characterization revealed the presence of physical crosslinking, without the formation of new chemical bonds. MSC secretome containing FGF-2 was visually observed to be absorbed and released from the hydrogel sponge matrix. However, ELISA testing revealed polymer interference that compromised the accuracy of FGF-2 quantification, necessitating the use of alternative, more specific methods for detecting FGF-2 within the solid matrix.

## 5. ACKNOWLEDGMENT

The authors express their sincere gratitude to the Faculty of Pharmacy, Universitas Andalas for the grand research (Penelitian Dosen Pemula AA/Lektor Contract No. 25/UN16.10.D/PJ.01/2025).

## REFERENCES

American Society for Testing and Materials (2016). ASTM D638-14: Standard Practice for Preparation of Metallographic Specimens

Bal-Ozturk, A., O. Karal-Yilmaz, Z. P. Akguner, S. Aksu, A. Tas, and H. Olmez (2019). Sponge-Like Chitosan-Based Nanostructured Antibacterial Material as a Topical Hemostat. *Journal of Applied Polymer Science*, **136**(19); 1–10

Caplan, A. I. (2018). Mesenchymal Stem Cells in Regenerative Medicine. In *Principles of Regenerative Medicine*, 219-227. Elsevier Inc.

Chu, D. T., T. N. T. Phuong, N. L. B. Tien, D. K. Tran, L. B. Minh, V. V. Thanh, P. G. Anh, V. H. Pham, and V. T. Nga (2019). Adipose Tissue Stem Cells for Therapy: An Update on the Progress of Isolation, Culture, Storage, and Clinical Application. *Journal of Clinical Medicine*, **8**(7); 917

Deshpande, R., M. Kanitkar, S. Kadam, K. Dixit, H. Chhabra, J. Bellare, S. Datar, and V. P. Kale (2018). Matrix-Entrapped Cellular Secretome Rescues Diabetes-Induced EPC Dysfunction and Accelerates Wound Healing in Diabetic Mice. *PLoS One*, **13**(8); e0202510

Dharmalingam, K. and R. Anandalakshmi (2019). Fabrication, Characterization and Drug Loading Efficiency of Citric Acid Crosslinked NaCMC–HPMC Hydrogel Films for Wound Healing Drug Delivery Applications. *International Journal of Biological Macromolecules*, **134**; 815–829

 

Du, J., Q. Zhu, J. Guo, J. Gu, J. Guo, Y. Wu, L. Ren, S. Yang, and J. Jiang (2025). Preparation and Characterization of Edible Films from Gelatin and Hydroxypropyl Methylcellulose/Sodium Carboxymethylcellulose. *Heliyon*, **11**(1); e41613

Durairaj, V., R. Kalpana, and V. Kumar (2024). Polyethylene Glycol Cross-Linked Hydrogel for Drug Absorption Properties. *Journal of Pharmacy and Bioallied Sciences*, **16**(Suppl 2); S1201–S1203

Elabscience Biotechnology Co., Ltd. (n.d.). Human bFGF/FGF2 (Basic Fibroblast Growth Factor) ELISA Kit (E-EL-H6042). Product Information from Elabscience Official Website. Sandwich ELISA Kit for in Vitro Quantitative Determination of Human bFGF/FGF2 Concentrations in Serum, Plasma and Other Biological Fluids. Product Details Retrieved from Elabscience website

Farooq, M., A. W. Khan, M. S. Kim, and S. Choi (2021). The Role of Fibroblast Growth Factor (FGF) Signaling in Tissue Repair and Regeneration. *Cells*, **10**; 3242

Feng, W. and Z. Wang (2023). Tailoring the Swelling-Shrinkable Behavior of Hydrogels for Biomedical Applications. *Advanced Science*, **10**(28); 1–41

Foo, J. B., Q. H. Looi, P. P. Chong, N. H. Hassan, G. E. C. Yeo, C. Y. Ng, B. Koh, C. W. How, S. H. Lee, and J. X. Law (2021). Comparing the Therapeutic Potential of Stem Cells and Their Secretory Products in Regenerative Medicine. *Stem Cells International*, (1); 2616807

Francesko, A., P. Petkova, and T. Tzanov (2018). Hydrogel Dressings for Advanced Wound Management. *Current Medicinal Chemistry*, **25**(41); 5782–5797

Ghorpade, V. S., A. V. Yadav, and R. J. Dias (2016). Citric Acid Crosslinked Cyclodextrin/Hydroxypropyl Methylcellulose Hydrogel Films for Hydrophobic Drug Delivery. *International Journal of Biological Macromolecules*, **93**; 75–86

Ibrahim, R., H. Mndlovu, P. Kumar, S. A. Adeyemi, and Y. E. Choonara (2022). Cell Secretome Strategies for Controlled Drug Delivery and Wound-Healing Applications. *Polymers*, **14**(14)

Jiang, X., M. Wu, J. Albo, and Q. Rao (2021). Non-Specific Binding and Cross-Reaction of ELISA: A Case Study of Porcine Hemoglobin Detection. *Foods*, **10**(8); 1–17

Kwon, J. W., C. Savitri, B. An, S. W. Yang, and K. Park (2023). Mesenchymal Stem Cell-Derived Secretome-Enriched Alginate/Extracellular Matrix Hydrogel Patch Accelerates Skin Wound Healing. *Biomaterials Research*, **27**(1); 1–20

Lai, C. P., O. Mardini, M. Ericsson, S. Prabhakar, C. Maguire, C. W. John, T. A. Bakhos, and X. O. Breakefield (2014). Dynamic Biodistribution of Extracellular Vesicles In Vivo Using a Multimodal Imaging Reporter. *ACS Nano*, **8**(1); 483–494

Li, Q., S. Gong, W. Yao, Z. Yang, R. Wang, Z. Yu, and M. Wei (2021). Exosome-Loaded Genipin Crosslinked Hydrogel Facilitates Full-Thickness Cutaneous Wound Healing in Rat Animal Model. *Drug Delivery*, **28**(1); 884–893

Li, Y., C. Zhu, D. Fan, R. Fu, P. Ma, Z. Duan, X. Li, H. Lei, and L. Chi (2020). Construction of Porous Sponge-Like PVA-CMC-PEG Hydrogels with pH-Sensitivity via Phase Separation for Wound Dressing. *International Journal of Polymeric Materials and Polymeric Biomaterials*, **69**(8); 505–515

Liu, K., T. Veenendaal, M. Wiendels, A. M. Ruiz-Zapata, J. van Laar, R. Kyranas, H. Enting, B. van Cranenbroek, H. J. P. M. Koenen, S. M. Mihaila, E. Oosterwijk, and P. H. J. Kouwer (2020). Synthetic Extracellular Matrices as a Toolbox to Tune Stem Cell Secretome. *ACS Applied Materials & Interfaces*, **12**(51); 56723–56730

Marlina, R. Pradifta, H. Lucida, I. R. Sudji, H. N. Salsabila, N. Elida, and P. A. Namira (2023). Formulation of Mesenchymal Stem Cell Secretome as Antiaging Cream. *International Journal of Applied Pharmaceutics*, **15**(Special Issue 1); 45–50

Ng, K. W., P. A. Torzilli, R. F. Warren, and S. A. Maher (2014). Characterization of a Macroporous Polyvinyl Alcohol Scaffold for the Repair of Focal Articular Cartilage Defects. *Journal of Tissue Engineering and Regenerative Medicine*, **8**(1); 164–168

Nooshabadi, V. T., M. Khanmohamadi, E. Valipour, S. Mahdipour, A. Salati, Z. V. Malekshahi, S. Shafei, E. Amini, S. Farzamfar, and J. Ai (2020). Impact of Exosome-Loaded Chitosan Hydrogel in Wound Repair and Layered Dermal Reconstitution in Mice Animal Model. *Journal of Biomedical Materials Research Part A*, **108**(11); 2138–2149

Pandey, A., M. Momin, and A. Chando (2020). Silver Sulfadiazine-Loaded Breathable Hydrogel Sponge for Wound Healing. *Drug Metabolism and Personalized Therapy*, **35**(3); 13

Podhorská, B., M. Vetrík, E. Chylíková-Krumbholcová, L. Kománková, N. R. Banafshehvaragh, M. Šlouf, M. Dušková-Smrčková, and O. Janoušková (2020). Revealing the True Morphological Structure of Macroporous Soft Hydrogels for Tissue Engineering. *Applied Sciences*, **10**(19); 5–15

Qiao, L., Y. Liang, J. Chen, Y. Huang, S. A. Alsareii, A. M. Alamri, F. A. Harraz, and B. Guo (2023). Antibacterial Conductive Self-Healing Hydrogel Wound Dressing with Dual Dynamic Bonds Promotes Infected Wound Healing. *Bioactive Materials*, **30**; 129–141

Robert, A. W., F. A. Gomes, M. P. Rode, M. M. da Silva, M. B. da R. Veleirinho, M. Maraschin, L. Hayashi, G. W. Calloni, and M. A. Stimamiglio (2019). The Skin Regeneration Potential of a Pro-Angiogenic Secretome from Human Skin-Derived Multipotent Stromal Cells. *Journal of Tissue Engineering*, **10**; 2041731419833391

Shi, Q., Z. Qian, D. Liu, J. Sun, X. Wang, H. Liu, J. Xu, and X. Guo (2017). GMSC-Derived Exosomes Combined with a Chitosan/Silk Hydrogel Sponge Accelerates Wound Healing in a Diabetic Rat Skin Defect Model. *Frontiers in Physiology*, **8**; 1–16

Song, X., C. Zhu, D. Fan, Y. Mi, X. Li, R. Z. Fu, Z. Duan,

 

Y. Wang, and R. R. Feng (2017). A Novel Human-Like Collagen Hydrogel Scaffold with Porous Structure and Sponge-Like Properties. *Polymers*, **9**(12); 1–16

Spicer, C. D. (2020). Hydrogel Scaffolds for Tissue Engineering: The Importance of Polymer Choice. *Polymer Chemistry*, **11**(2); 184–219

Suresh, K. S., S. Bhat, B. R. Guru, M. S. Muttigi, and R. N. Seetharam (2020). A Nanocomposite Hydrogel Delivery System for Mesenchymal Stromal Cell Secretome. *Stem Cell Research & Therapy*, **11**(1); 1–14

Tate, J. and G. Ward (2004). Interferences in Immunoassay. *Clinical Biochemistry Reviews*, **25**(2); 105–120

Van De Sandt, J. J. M., J. A. Van Burgsteden, S. Cage, P. L. Carmichael, I. Dick, S. Kenyon, G. Korinth, F. Larese, J. C. Limasset, W. J. M. Maas, L. Montomoli, J. B. Nielsen, J. P. Payan, E. Robinson, P. Sartorelli, K. H. Schaller, S. C. Wilkinson, and F. M. Williams (2004). In Vitro Predictions of Skin Absorption of Caffeine, Testosterone, and Benzoic Acid: A Multi-Centre Comparison Study. *Regulatory Toxicology and Pharmacology*, **39**(3); 271–281

Wang, C., M. Wang, T. Xu, X. Zhang, C. Lin, W. Gao, H. Xu, B. Lei, and C. Mao (2019). Engineering Bioactive Self-Healing Antibacterial Exosomes Hydrogel for Promoting Chronic Diabetic Wound Healing and Complete Skin Regeneration. *Theranostics*, **9**(1); 65–76

Widowati, W., D. Rahmat, A. Faried, I. M. Nainggolan, D. Priyandoko, T. L. Wargasetia, V. K. Sugiaman, D. N. Triharsiwi, S. Qlintang, H. Murti, R. Azis, and J. Jeffrey (2025). Potential of Secretome Hydrogel for Wound Healing in LPS- and Scratch-Induced BJ Cells as an Inflammation Model. *Science and Technology Indonesia*, **10**(4); 1242–1254

Yao, T. and Y. Asayama (2017). Animal-Cell Culture Media: History, Characteristics, and Current Issues. *Reproductive Medicine and Biology*, **16**(2); 99–117

Yim, H. E., D. S. Kim, H. C. Chung, B. Shing, K. H. Moon, S. K. George, M. W. Kim, A. Atala, J. H. Kim, I. K. Ko, and J. J. Yoo (2019). Controlled Delivery of Stem Cell-Derived Trophic Factors Accelerates Kidney Repair After Renal Ischemia-Reperfusion Injury in Rats. *Stem Cells Translational Medicine*, **8**(9); 959–970

You, T., Q. You, X. Feng, H. Li, B. Yi, and H. Xu (2024). A Novel Approach to Wound Healing: Green Synthetic Nano-Zinc Oxide Embedded with Sodium Alginate and Polyvinyl Alcohol Hydrogels for Dressings. *International Journal of Pharmaceutics*, **654**; 1–11

Yu, C., Y. Lu, J. Pang, and L. Li (2024). A Hemostatic Sponge Derived from Chitosan and Hydroxypropylmethylcellulose. *Journal of the Mechanical Behavior of Biomedical Materials*, **150**

Zhang, J., Z. Yang, C. Li, Y. Dou, Y. Li, T. Thote, D. A. Wang, and Z. Ge (2013). Cells Behave Distinctly Within Sponges and Hydrogels Due to Differences of Internal Structure. *Tissue Engineering Part A*, **19**(19–20); 2166–2175

Zhang, M. and X. Zhao (2020). Alginate Hydrogel Dressings for Advanced Wound Management. *International Journal of Biological Macromolecules*, **162**; 1414–1428

Zhang, Y., Y. Zheng, F. Shu, R. Zhou, B. Bao, S. Xiao, K. Li, Q. Lin, L. Zhu, and Z. Xia (2022). In Situ-Formed Adhesive Hyaluronic Acid Hydrogel with Prolonged Amnion-Derived Conditioned Medium Release for Diabetic Wound Repair. *Carbohydrate Polymers*, **276**; 118752

 